The influence of dispersal on a predator-prey system with two habitats

P. Gramlich[1], S.J.Plitzko[1], L.Rudolf[1], B.Drossel[1], T.Gross[1]

Abstract

Dispersal between different habitats influences the dynamics and stability of populations considerably. Furthermore, these effects depend on the local interactions of a population with other species. Here, we perform a general and comprehensive study of the simplest possible system that includes dispersal and local interactions, namely a 2-patch 2-species system. We evaluate the impact of dispersal on stability and on the occurrence of bifurcations, including pattern forming bifurcations that lead to spatial heterogeneity, in 19 different classes of models with the help of the generalized modelling approach. We find that dispersal often destabilizes equilibria, but it can stabilize them if it increases population losses. If dispersal is nonrandom, i.e. if emigration or immigration rates depend on population densities, the correlation of stability with migration rates is positive in part of the models. We also find that many systems show all four types of bifurcations and that antisynchronous oscillations occur mostly with nonrandom dispersal.

Keywords:
Generalized modelling, Metapopulations, Adaptive migration,

1. Introduction

In ecology both the exploration of dynamical models of food webs (Pascual and Dunne, 2005; Thompson et al., 2012; Rooney and McCann, 2012) and the study of spatial metapopulations(Holland and Hastings, 2008; Ristl et al., 2014; Hanski and Gaggiotti, 2004) are well established lines of research.

Email addresses: gramlich@fkp.tu-darmstadt.de (P. Gramlich), plitzko@fkp.tu-darmstadt.de (S.J.Plitzko), rudolflars@googlemail.com (L.Rudolf), drossel@fkp.tu-darmstadt.de (B.Drossel), thilo2gross@gmail.com (T.Gross)

The two modelling approaches emphasize different aspects of ecological dynamics that are both relevant for most species: the dispersal between different habitat patches and tropic interactions with other species. Yet, models that combine dispersal with trophic dynamics have only recently begun to appear.

In the following we refer to models that include both trophic interactions and dispersal between spatial patches as meta-foodwebs. An elegant highly-simplified meta-foodweb model was proposed by Pillai (Pillai et al., 2011). More detailed dynamical models were proposed in Abrams and Ruokolainen (2011), Abdllaoui et al. (2007) and Jansen (2001), to name a few. The different models draw motivation from different biological examples and hence make different modelling choices regarding the nature of dispersal and other aspects of the system. For example Jansen (2001) assumes diffusive dispersal between patches which is a rather accurate model for simple lifeforms as bacteria whereas Abrams and Ruokolainen (2011) make dispersal dependent on the species fitness on different patches, allowing the species to actively search for the best growth conditions which requires animals that somehow perceive the other patch and are able of active movement. Though these particular examples only describe two patches, conclusions from multi-patch models are often consistent with those from two-patch models (Jansen and de Roos, 2000), and therefore the insights gained from 2-patch systems have wider applications.

In the literature different assumptions are made regarding the functional forms of the number of emigrants from a given habitat patch, the choice of destination, the proportion of survivors that arrive as immigrants in the destination patch and the settlement success (Amarasekare, 2008; Armsworth and Roughgarden, 2008; Rowell, 2010). In the simplest case a fixed proportion of the population emigrates per unit time and instantaneously and losslessly settles in a randomly chosen neighbouring patch (Leibold et al., 2004). This type of migration is usually called "random dispersal" or "diffusive migration", and often leads to a synchronisation of the population dynamics of the two patches (Goldwyn and Hastings, 2008; Jansen, 2001). Examples for non-random dispersal are predator evasion and predator pursuit (Li et al., 2005), or a migration rate that is proportional to the difference in growth rates between two patches (Abrams and Ruokolainen, 2011).

With such adaptive dispersal, antisynchronous oscillations of the two patches are observed, which increase metapopulation persistence. While synchronisation does not necessarily require strong dispersal (Liebhold et al., 2004), more rapid dispersal is more likely to synchronize populations. The

less similar populations are the less likely is it that dispersal is synchronizing (Esa Ranta and Lundberg, 1998). Other authors find that increased dispersal can decrease synchrony in population dynamics depending on the interactions between migrating species (Koelle and Vandermeer, 2005).

An investigation based on the generalized modelling approach (Tromeur et al., 2013) found that costly dispersal and social fencing are stabilizing, while positive density dependence and settlement facilitation reduce stability. Other papers have shown that costly dispersal might be destabilizing to a metapopulation with homogeneous patches (va Kisdi, 2010) so the specific mechanisms appear to be of importance. The effects of dispersal on stability can depend not only on the type but also on the intensity of the dispersal (Briggs and Hoopes, 2004).

While much progress has been made for specific example systems, a broad and general understanding of how different factors impact the stability of meta-foodwebs is still lacking. For instance it is unclear under which conditions dispersal has a stabilizing impact. One also has to ask what types of instabilities are typically encountered in meta-foodwebs. The study of foodwebs has provided abundant examples of two basic mechanisms of instability. The saddle-node bifurcation, which can lead to the relatively sudden collapse of populations, and the Hopf bifurcation, which gives rise (to at least transient) oscillations. In meta-foodwebs both of these instabilities can occur in two variants. The first off these affects all patches equally, and is thus closely analogous to the bifurcations in non-spatial food web models. In the second type different patches are affected differently. They are thus reminiscent of pattern-forming instabilities such as the Turing and wave-instabilities, that known from systems of partial differential equations. While also these bifurcations lead to instability, their impact on the overall population density is less pronounced, and they act as drivers of heterogeneity, which, in the long run, might benefit the system.

In order to gain an overview of the possible dynamical patterns of a system and their requirements, the generalized modelling approach (Gross and Feudel, 2006; Yeakel et al., 2011; Gross et al., 2009), which is based on a linear stability analysis of equilibria, is particularly powerful. The idea behind this approach is to consider models where the kinetics of some processes have not been restricted to specific functional forms. Considering a model with a specific structure, but containing general functions, allows capturing well-known insights into the structure of the system, without requiring often questionable assumptions on the exact form of kinetics. Further advantages

are a short computation time and ease of biological interpretation.

In this paper, we investigate the dynamics of two species on two identical patches using the generalized modelling approach. We are able to analyse a broad class of models that includes several previously studied systems as special cases. We focus on the effect of the type and strength of migration on the stability and the dynamics of the system. We find migration to be destabilizing in almost all cases. Complex migration rules allow for a stabilizing influence of dispersal and can produce saddle-node and Hopf bifurcations and spatial-pattern forming bifurcations.

2. Model

2.1. Generalized modelling formulation

We consider a system consisting of two habitat patches, where each patch i can potentially sustain a prey population X_i and a predator population Y_i. We assume a homogeneous system, such that both patches are described by identical parameter values. The population dynamics are described by

$$\begin{aligned}
\dot{X}_1 &= G(X_1) - K(X_1) - F(X_1, Y_1) \\
&\quad + \eta^X E^X(X_2, Y_2, X_1, Y_1) - E^X(X_1, Y_1, X_2, Y_2) \\
\dot{Y}_2 &= \lambda F(X_1, Y_1) - D(Y_1) \\
&\quad + \eta^Y E^Y(X_2, Y_2, X_1, Y_1) - E^Y(X_1, Y_1, X_2, Y_2) \\
\dot{X}_2 &= G(X_2) - M(X_2) - F(X_2, Y_2) \\
&\quad + \eta^X E^X(X_1, Y_1, X_2, Y_2) - E^X(X_2, Y_2, X_1, Y_1) \\
\dot{Y}_2 &= \lambda F(X_2, Y_2) - D(Y_2) \\
&\quad + \eta^Y E^Y(X_1, Y_1, X_2, Y_2) - E^Y(X_2, Y_2, X_1, Y_1)\,,
\end{aligned} \tag{1}$$

where we used the dot over a variable to indicate the temporal derivative. The variables are in arbitrary units. For the purpose of this paper we will assume that they describe the system in terms of carbon biomass density, However, the same equations also apply to other measures of population, such as abundance. The prey population density changes due to a growth rate $G(X_i)$, a respiration/mortality rate $K(X_i)$, and a rate of biomass loss by predation $F(X_i, Y_i)$. Predator populations have a growth term $\lambda F(X_i, Y_i)$, with the prefactor λ describing the efficiency of the energy conversion. The respiration/mortality rate of the predator is given by $D(Y_i)$. The rate of emigration is $E^U(\mathbf{X},\mathbf{Y})$ for both species $U = X, Y$ and the migration loss factor

is η^U. In the most general case, emigration rates depend on all four populations. The case where the emigration rate of population U_i is proportional to E_i and independent of other variables corresponds to diffusive migration, otherwise we get different versions of adaptive migration.

Modes of the form Eqs. (1) can have multiple feasible steady states, depending one the choice of functional forms and parameter values. In the generalized model we cannot compute the steady states. However, a central insight is that we can still compute conditions for the stability of steady states and express them in the form of meaningful ecological parameters. For this purpose we consider an arbitrary feasible, but not necessarily stable state.

The normalized biomasses are

$$x_i = \frac{X_i}{X^*}\,, \quad y_i = \frac{Y_i}{Y^*}\,, \tag{2}$$

and the normalized functions are

$$h(\mathbf{x},\mathbf{y}) = \frac{H(\mathbf{X},\mathbf{Y})}{H(\mathbf{X}^*,\mathbf{Y}^*)} \equiv \frac{H(\mathbf{X},\mathbf{Y})}{H^*} \tag{3}$$

with $H = E, F, G, K$ and the asterisk (*) is used to denote the values of variables and functions in this steady state under consideration.

In terms of these normalized quantities, Eqs. (1) take the form

$$\begin{aligned}
\dot{x}_1 &= \frac{G^*}{X^*}g(x_1) - \frac{K^*}{X^*}k(x_1) - \frac{F^*}{X^*}f(x_1,y_1) + \frac{E^{X*}\eta^X}{X^*}e^X(\mathbf{x},\mathbf{y}) - \frac{E^{X*}}{X^*}e^X(\mathbf{x},\mathbf{y}) \\
\dot{y}_1 &= \frac{\lambda F^*}{Y^*}f(x_1,y_1) - \frac{D^*}{Y^*}d(y_1) + \frac{E^{Y*}\eta^Y}{Y^*}e^Y(\mathbf{x},\mathbf{y}) - \frac{E^{Y*}}{Y^*}e^Y(\mathbf{x},\mathbf{y}) \qquad (4) \\
\dot{x}_2 &= \frac{G^*}{X^*}g(x_2) - \frac{K^*}{X^*}k(x_2) - \frac{F^*}{X^*}f(x_2,y_2) + \frac{E^{X*}\eta^X}{X^*}e^X(\mathbf{x},\mathbf{y}) - \frac{E^{X*}}{X^*}e^X(\mathbf{x},\mathbf{y}) \\
\dot{y}_2 &= \frac{\lambda F^*}{Y^*}f(x_2,y_2) - \frac{D^*}{Y^*}d(y_2) + \frac{E^{Y*}\eta^Y}{Y^*}e^Y(\mathbf{x},\mathbf{y}) - \frac{E^{Y*}}{Y^*}e^Y(\mathbf{x},\mathbf{y}).
\end{aligned}$$

It is now useful to identify the total biomass turnover rate of the species, which we can write as

$$\alpha^X = \frac{G^*}{X^*} + \frac{E^{X*}\eta^X}{X^*} = \frac{K^*}{X^*} + \frac{F^*}{X^*} + \frac{E^{X*}}{X^*}\,, \tag{5}$$

$$\alpha^Y = \frac{\lambda F^*}{Y^*} + \frac{E^{Y*}\eta^Y}{Y^*} = \frac{D^*}{Y^*} + \frac{E^{Y*}}{Y^*}\,. \tag{6}$$

For instance if the variables describe abundances then the parameter $\alpha^X$is the total turnover rate for the prey in a patch. For instance a value of 0.25/year would indicate that an individual spends on average 4 years in the patch before either dying or emigrating.

In general it is advantageous to measure time in terms of the prey turnover α^X. In this rescaled time units the turnover rate of the prey is 1 and the turnover rate of the predator is

$$\alpha = \frac{\alpha^Y}{\alpha^X}\,. \tag{7}$$

Furthermore, we define the scale parameters δ, ν and ρ and their complements

$$\begin{aligned}
\delta &= \frac{1}{\alpha^X \rho^X}\frac{F^*}{X^*}\,, \qquad \tilde{\delta} = (1-\delta) = \frac{1}{\alpha^X \rho^X}\frac{K^*}{X^*}\,, && (8)\\
\nu^U &= \frac{1}{\alpha^U}\frac{E^{U*}\eta^U}{U^*}\,, \qquad \tilde{\nu}^U = (1-\nu^U) = \frac{1}{\alpha^U}\frac{\{G^*;\lambda F^*\}}{U^*}\,, && (9)\\
\rho^U &= \frac{1}{\alpha^U}\frac{E^{U*}\tilde{\eta}^U}{U^*}\,, \qquad \tilde{\rho}^U = (1-\rho^U) = \frac{1}{\alpha^U}\frac{\{K^*+F^*;D^*\}}{U^*}\,. && (10)
\end{aligned}$$

All of these parameters describe the branching of the biomass flow. The parameter δ denotes the proportion of energy intake of the prey that is eventually lost again due to respiration or mortality, whereas the $\tilde{\delta}$ is the proportion of the energy intake that is eventually lost due to predation. The parameters ν and $\tilde{\nu}$ denote the relative contributions of migration and feeding to the total gain, respectively. The parameters ρ and $\tilde{\rho}$ are the counterpart to ν and $\tilde{\nu}$ and denote the relative loss by emigration and by the within-patch processes (respiration/mortality and predation).

Using the definitions above we can write Eq. (4) as

$$\begin{aligned}
\dot{x}_1 &= \alpha^X[\tilde{\nu}^X g(x_1) - \tilde{\rho}_1^X \tilde{\delta} m(x_1) - \tilde{\rho}^X \delta f(x_1,y_1) + \nu^X e^X(\mathbf{x},\mathbf{y}) - \rho^X e^X(\mathbf{x},\mathbf{y})]\\
\dot{y}_1 &= \alpha^Y[\tilde{\nu}^Y f(x_1,y_1) - \tilde{\rho}^Y d(y_1) + \nu^Y e^Y(\mathbf{x},\mathbf{y}) - \rho^Y e^Y(\mathbf{x},\mathbf{y})] \qquad (11)\\
\dot{x}_2 &= \alpha^X[\tilde{\nu}^X g(x_2) - \tilde{\rho}^X \tilde{\delta} m(x_2) - \tilde{\rho}^X \delta f(x_2,y_2) + \nu^X e^X(\mathbf{x},\mathbf{y}) - \rho^X e^X(\mathbf{x},\mathbf{y})]\\
\dot{y}_2 &= \alpha^Y[\tilde{\nu}^Y f(x_2,y_2) - \tilde{\rho}^Y d(y_2) + \nu^Y e^Y(\mathbf{x},\mathbf{y}) - \rho^Y e^Y(\mathbf{x},\mathbf{y})].
\end{aligned}$$

For analysing the stability we linearise the system around the steady state under consideration. In the normalized system the steady state is at x=y=1. The linearisation can then be expressed in terms of the Jacobian matrix. For

a system of four dynamical variables this is a 4×4 matrix. defined by

$$J_{i,j} = \left. \frac{\partial \dot{V}_i}{\partial V_j} \right|_* , \tag{12}$$

where $V = (x_1, y_1, x_2, y_2)$ is the set of state variables and $|_*$ indicates that the derivatives are evaluated in the steady state (1,1,1,1).

For the case of a system with two identical patches the 4×4 matrix can be written as a block matrix

$$J = \begin{pmatrix} L & M \\ M & L \end{pmatrix} \tag{13}$$

with

$$L = \begin{pmatrix} 1 & 0 \\ 0 & \alpha \end{pmatrix} \begin{pmatrix} \tilde{\nu}^X \phi - \tilde{\rho}^X \tilde{\delta} \mu^X - \tilde{\rho}^X \delta \gamma + \nu^X \hat{\omega}^X - \rho^X \omega^X & -\tilde{\rho}^X \delta \psi + \nu^X \hat{\kappa}^X - \rho^X \kappa^X \\ \tilde{\nu}^Y \gamma + \nu^Y \hat{\kappa}^Y - \rho^Y \kappa^Y & \tilde{\nu}^Y \psi - \tilde{\rho}^Y \mu^Y + \nu^Y \hat{\omega}^Y - \rho^Y \omega^Y \end{pmatrix} \tag{14}$$

and

$$M = \begin{pmatrix} 1 & 0 \\ 0 & \alpha \end{pmatrix} \begin{pmatrix} \nu^X \omega^X - \rho^X \hat{\omega}^X & \nu^X \kappa^X - \rho^X \hat{\kappa}^X \\ \nu^Y \kappa^Y - \rho^Y \hat{\kappa}^Y & \nu^Y \omega^Y - \rho^Y \hat{\omega}^Y \end{pmatrix} . \tag{15}$$

We note that the matrix L captures the effects of in-patch dynamics whereas the matrix M captures between-patch dynamics. The new parameters in these matrices are called *exponent parameters*, and they are the derivatives of the population dynamic functions with respect to the prey or predator populations. The definitions of the exponent parameters are

$$
\begin{aligned}
\phi &:= \left.\frac{\partial g(x)}{\partial x}\right|_*, \qquad \mu^X := \left.\frac{\partial m(x)}{\partial x}\right|_*, \qquad \mu^Y := \left.\frac{\partial d(y)}{\partial y}\right|_*, \\
\gamma &:= \left.\frac{\partial f(x,y)}{\partial x}\right|_*, \qquad \psi := \left.\frac{\partial f(x,y)}{\partial y}\right|_*, \\
\hat{\omega}^X &:= \left.\frac{\partial e^X(\mathbf{x},\mathbf{y})}{\partial x}\right|_*, \qquad \omega^X := \left.\frac{\partial e^X(\mathbf{x},\mathbf{y})}{\partial x}\right|_*, \\
\hat{\kappa}^X &:= \left.\frac{\partial e^X(\mathbf{x},\mathbf{y})}{\partial y}\right|_*, \qquad \kappa^X := \left.\frac{\partial e^X(\mathbf{x},\mathbf{y})}{\partial y}\right|_*, \\
\hat{\omega}^Y &:= \left.\frac{\partial e^Y(\mathbf{x},\mathbf{y})}{\partial y}\right|_*, \qquad \omega^Y := \left.\frac{\partial e^Y(\mathbf{x},\mathbf{y})}{\partial y}\right|_*, \\
\hat{\kappa}^Y &:= \left.\frac{\partial e^Y(\mathbf{x},\mathbf{y})}{\partial x}\right|_*, \qquad \kappa^Y := \left.\frac{\partial e^Y(\mathbf{x},\mathbf{y})}{\partial x}\right|_*.
\end{aligned}
\tag{16}
$$

The exponent parameters are so-called elasticities, i.e. they are logarithmic derivatives of the original functions. For example

$$
\phi = \left.\frac{\partial g(x)}{\partial x}\right|_* = \left.\frac{\partial \log(G(X))}{\partial \log(X)}\right|_*. \tag{17}
$$

Such logarithmic derivatives have a number of advantageous properties. Elasticities as a measure of nonlinearity where first introduced in the 1920 in economic theory, because of their statistical properties which allows them to be estimated precisely based on limited noisy data. For the same reason these parameters are now commonly used in metabolic control theory.

In generalized models we use elasticities mainly because they allow for an intuitive interpretation: For any linear function, say $G(X) = AX$, the corresponding elasticity $\partial\log(G(X))/\partial\log(X)|_1$ is 1, regardless of the slope A. More generally for any power law $G/(X) = AX^p$ the elasticity is the power law exponent p. For more complex functions the elasticity provides an intuitive measure of the saturation of the underlying process. For example for the Holling type-II kinetics the corresponding elasticity is close to 1 in the linear regime at low prey density, but becomes 0 in the limit of predator saturation at high prey density.

The ω and κ are the migration exponent parameters, where ω describes the dependence of the emigration on the density of species of the emigrating individuals, whereas κ describes the dependence of emigration on the density

Parameter	Interpretation	Range	Examples
ϕ	Elasticity of the gain function	$[0, 1]$	0: growth independent of population size, e.g. due to nutrient limitation, 1: growth prop. to population density
μ^X	Sensitivity of prey mortality to prey population	$[1, 2]$	1: constant mortality 2: mortality proportional to density, e.g. due to diseases
μ^Y	Sensitivity of predator mortality to predator population	$[1, 2]$	same as for prey
γ	Sensitivity of predation gain to prey population	$[0, 2]$	Holling type functions: value close to 1 for small prey population, low value for large pop. due to saturation
ψ	Sensitivity of predation gain to predator population	$[0, 1]$	1: No predator competition, lower values are due to predator interference

Table 1: The five exponent parameters, their meaning, and the range of their values in our computations.

of the other species in the patch, respectively. The parameters with a hat $\hat{\omega}, \hat{\kappa}$ are defined analogously but describe the dependence on the densities in the destination patch. Different types of adaptive migration imply different parameter ranges for these exponent parameters. Simple diffusive migration for species U means $\omega^U = 1$ and when the emigration rate increases with population size we get an exponent $\omega^U > 1$. In predator evasion, prey emigration is increased with predator density, which means a value $\kappa^X > 0$. In predator pursuit, predator emigration is decreased with prey density, which means $\kappa^Y < 0$.

The remaining five parameters (first five in Eq. 16) describe the elasticity of the local (within-patch) processes. These parameters have been discussed extensively in previous work (e.g. Gross and Feudel (2006)). Hence, we summarize their interpretation in Tab. 1.

2.2. Linear stability, eigenvalues, and bifurcations

In order to evaluate the stability of an equilibrium, we have to calculate the eigenvalues of the Jacobian at the steady state. Due to the symmetric block structure of the Jacobian, the eigenvalue equation can be solved with the ansatz(MacArthur et al., 2008)

$$\begin{pmatrix} L_1 & L_2 & M_1 & M_2 \\ L_3 & L_4 & M_3 & M_3 \\ M_1 & M_2 & L_1 & L_2 \\ M_3 & M_4 & L_3 & L_4 \end{pmatrix} \begin{pmatrix} \xi_1 \\ \xi_2 \\ \pm\xi_1 \\ \pm\xi_2 \end{pmatrix} = \lambda \begin{pmatrix} \xi_1 \\ \xi_2 \\ \pm\xi_1 \\ \pm\xi_2 \end{pmatrix},$$

with L_i and M_i denoting the matrix elements of L and M. This is equivalent to solving the 2x2 problem

$$\begin{pmatrix} L_1 \pm M_1 & L_2 \pm M_2 \\ L_3 \pm M_3 & L_4 \pm M_4 \end{pmatrix} \begin{pmatrix} \xi_1^{\pm} \\ \xi_2^{\pm} \end{pmatrix} = \lambda \begin{pmatrix} \xi_1^{\pm} \\ \xi_2^{\pm} \end{pmatrix}.$$

Every solution of the eigenvalue equation describes an eigenmode of the system, i.e. a specific perturbation that retains its shape while it grows or declines in time. For the plus sign, the eigenvector components relating to the two patches are identical, for the minus sign, they point in opposite directions.

The equilibrium is stable if the real parts of all eigenvalues are negative. The eigenvalues for a 2x2 matrix J' can be written in terms of trace (T) and the determinant (Δ) of the matrix as

$$\lambda_{1,2} = \frac{1}{2}T(J') \pm \sqrt{\frac{1}{4}T(J')^2 - \Delta(J')}\,. \tag{18}$$

For stability we need the real part of both eigenvalues to be stable, which is the case if the trace is negative and the determinant is positive. These criteria must be satisfied for both matrices $L \pm M$ (below denoted by the index "+" for "L+M" and "-" for "L-M") for the equilibrium to be stable. As parameters are changed, a stable equilibrium can become unstable when the change causes an eigenvalue to acquire a positive real part.. We can distinguish 4 different bifurcation scenarios.

Let us first consider the "$J_+ = L+M$" case. Instabilities that are detected by the analysis of this matrix affect both patches equally and in synchrony. First, stability of the steady state can be lost in a saddle-node bifurcation,

which occurs when $\Delta(J_+) = 0$ and $T(J_+) < 0$ while both eigenvalues of J_- have a negative real part. In this bifurcation a sudden change in the population densities occurs, which most likely results in the collapse of one or both populations in both patches simultaneously.

The second fundamental bifurcation in which stability can be lost is the Hopf bifurcation. This bifurcation occurs when $T(J_+) = 0$ and $\Delta(J_+) > 0$ while the eigenvalues of J_- have a negative real part. The Hopf bifurcations detected in the L+M matrix affect the patches identically, such that they lead to synchronous oscillations. From the study on non-spatial predator-prey systems it is well known that oscillation amplitudes can grow rapidly after the bifurcation, leading to subsequent extinctions (Rosenzweig and MacArthur, 1963).

Let us now consider the $J_- = L - M$ matrix. Bifurcations detected in this matrix affect the two patches diametrically. Again, stability can be lost either in a saddle-node or in a Hopf bifurcation. However, now the Saddle-node bifurcation leads to a shift where each population increases in one patch and decreases in the other.This occurs when $\Delta(J_-) = 0$ and $T(J_-) < 0$ and both eigenvalues of J_+ have a negative real part.

A Hopf bifurcation detected in the L-M matrix leads to anti-synchronous oscillations. While this can lead to large amplitude oscillations in both individual patches, the overall biomass in the system will stay nearly constant as the loss in one patch is compensated by gains in the other.

Both bifurcations occurring in the L-M matrix can be considered as *pattern-forming* bifurcations that create spatial heterogeneity. In fact, the saddle-node bifurcation in the L-M case is closely reminiscent of the Turing bifurcation in systems of partial differential equations, which gives rise to stationary patterns. The Hopf bifurcation is reminiscent of the wave instability bifurcation, in partial differential equations, which leads to travelling waves. This "wave instability" occurs at $T(J_-) = 0$ and $\Delta(J_-) > 0$ with both eigenvalues of J_+ having a negative real part.

In the following we will use the terms Hopf and saddle-node bifurcation only for the corresponding bifurcations from the L+M matrix. For simplicity we will denote the respective bifurcations in the L-M system as Turing and wave instability. We emphasize that this is a loose usage of the bifurcation names, that we adopt here as it leads to the right ecological intuition although

it is not strictly mathematically justified[1].

2.3. Classes of models studied in the following

In order to evaluate the proportion of stable systems and the frequency of the different types of bifurcations, we need to specify intervals for the exponent parameters and the scale parameters. Different classes of models are characterized by different choices for these intervals. We use several models from the existing literature as well as more general models. All these models are listed in Tab. 2.

[1]Strictly, a bifurcation is of a given type only if it can be reduced to the types normal form. For instance the saddle-node bifurcation observed in the L-M system can be reduced to the saddle-node normal form but not to the Turing normal form. So strictly it is a saddle-node and not a Turing bifurcation. Still one can justify denoting this bifurcation as 'Turing' as follows: The bifurcation would not change fundamentally when we considered a system with more than two patches. The bifurcation would then be governed by a matrix that is closely reminiscent of the network laplacian, which in turn can be seen as a discretization of the real space laplacian on a complex network. In this sense even the 2-patch system can be interpreted as a discretization of an underlying continuous space in which the bifurcation would be a true Turing bifurcation.

Scen.	ϕ	δ	γ	ψ	μ^X	μ^Y	α	ν^X	ν^Y	ρ^X	ρ^Y	ω^X	ω^Y	$\hat{\omega}^X$	$\hat{\omega}^Y$	κ^X	κ^Y	$\hat{\kappa}^X$	$\hat{\kappa}^Y$
(1) Stand.	$[0;1]$	$[0;1]$	$[0;2]$	$[0;1]$	$[1;2]$	$[1;2]$	$[10^{-3};10^{1}]$	$[0;1]$	$[0;1]$	$[0;1]$	$[0;1]$	$[-2;2]$	$[-2;2]$	$[-2;2]$	$[-2;2]$	$[-2;2]$	$[-2;2]$	$[-2;2]$	$[-2;2]$
(1x) Stand.	$[0;1]$	$[0;1]$	$[0;2]$	$[0;1]$	$[1;2]$	$[1;2]$	$[10^{-3};10^{1}]$	$[0;1]$	$[0;1]$	0	0	$[-2;2]$	$[-2;2]$	$[-2;2]$	$[-2;2]$	$[-2;2]$	$[-2;2]$	$[-2;2]$	$[-2;2]$
(1z) Stand.	$[0;1]$	$[0;1]$	$[0;2]$	$[0;1]$	$[1;2]$	$[1;2]$	$[10^{-3};10^{1}]$	$[0;1]$	$[0;1]$	ν^X	ν^Y	$[-2;2]$	$[-2;2]$	$[-2;2]$	$[-2;2]$	$[-2;2]$	$[-2;2]$	$[-2;2]$	$[-2;2]$
(2) Diff	$[0;1]$	$[0;1]$	$[0;2]$	$[0;1]$	$[1;2]$	$[1;2]$	$[10^{-3};10^{1}]$	$[0;1]$	$[0;1]$	$[0;1]$	$[0;1]$	1	1	0	0	0	0	0	0
(2x) Diff	$[0;1]$	$[0;1]$	$[0;2]$	$[0;1]$	$[1;2]$	$[1;2]$	$[10^{-3};10^{1}]$	$[0;1]$	$[0;1]$	0	0	1	1	0	0	0	0	0	0
(2z) Diff	$[0;1]$	$[0;1]$	$[0;2]$	$[0;1]$	$[1;2]$	$[1;2]$	$[10^{-3};10^{1}]$	$[0;1]$	$[0;1]$	ν^X	ν^Y	1	1	0	0	0	0	0	0
(2y) Diff	$[0;1]$	$[0;1]$	$[0;2]$	$[0;1]$	$[1;2]$	$[1;2]$	$[10^{-3};10^{1}]$	$[0;1]$	0	ν^X	0	1	1	0	0	0	0	0	0
(3) Mchich	1	1	1	1	0	1	$[10^{-3};10^{1}]$	$[0;1]$	$[0;1]$	$[0;1]$	$[0;1]$	1	1	0	0	$[0;1]$	0	0	0
(3x) Mchich	1	1	1	1	0	1	$[10^{-3};10^{1}]$	$[0;1]$	$[0;1]$	0	0	1	1	0	0	$[0;1]$	0	0	0
(4) Jans95	1	$[0;1]$	$[0;1]$	1	2	1	$[10^{-3};10^{1}]$	$[0;1]$	$[0;1]$	$[0;1]$	$[0;1]$	1	1	0	0	0	0	0	0
(4x) Jans95	1	$[0;1]$	$[0;1]$	1	2	1	$[10^{-3};10^{1}]$	$[0;1]$	$[0;1]$	0	0	1	1	0	0	0	0	0	0
(4z) Jans95	1	$[0;1]$	$[0;1]$	1	2	1	$[10^{-3};10^{1}]$	$[0;1]$	$[0;1]$	ν^X	ν^Y	1	1	0	0	0	0	0	0
(5) Jans01	1	$[0;1]$	$[0;1]$	1	2	1	$[10^{-3};10^{1}]$	0	$[0;1]$	0	$[0;1]$	0	1	0	0	0	0	0	0
(5z) Jans01	1	$[0;1]$	$[0;1]$	1	2	1	$[10^{-3};10^{1}]$	0	$[0;1]$	0	ν^Y	0	1	0	0	0	0	0	0
(6) Huang	1	$[0;1]$	$[0;1]$	1	2	1	$[10^{-3};10^{1}]$	0	$[0;1]$	0	$[0;1]$	0	1	0	0	0	$-[0;1]$	0	0
(6R) Huang	1	$[0;1]$	$[0;1]$	1	2	1	$[10^{-3};10^{1}]$	0	$[0;1]$	0	$[0;1]$	0	1	0	0	0	$[0;1]$	0	0
(7) Abrams11	1	$[0;1]$	$[0;1]$	1	2	1	$[10^{-3};10^{1}]$	0	$[0;1]$	0	$[0;1]$	0	1	0	0	0	$-\hat{\kappa}^Y$	0	$[0;\frac{\lambda b}{4h}]$
(8) El Abdl.	1	$[0;1]$	1	1	2	1	$[10^{-3};10^{1}]$	$[0;1]$	$[0;1]$	$[0;1]$	$[0;1]$	1	1	0	0	1	-1	0	0
(9) Growth	$[0;1]$	$[0;1]$	$[0;2]$	$[0;1]$	$[1;2]$	$[1;2]$	$[10^{-3};10^{1}]$	$[0;1]$	$[0;1]$	$[0;1]$	$[0;1]$	ϕ	ψ	ϕ	ψ	γ	0	γ	0
(10) Growth2	1	$[0;1]$	$[0;1]$	1	2	1	$[10^{-3};10^{1}]$	$[0;1]$	$[0;1]$	$[0;1]$	$[0;1]$	ϕ	ψ	ϕ	ψ	γ	0	γ	0

Table 2: The different models ("scenarios") analysed in this paper. The models *Jan95*, *Jan01*, *Abrams11*, *Mchich ElAbdl.* can be found in V.A.A.Jansen (1995), Abdllaoui et al. (2007), Abrams and Ruokolainen (2011), Jansen (2001) and Mchich et al. (2007).*Stand* represents the most general scenario with a wide range of plausible parameters. *Diff* combines general local dynamics with diffusive migration. *Growth* couples growth rates and feeding terms to migration terms. *Jans95*, *Jans01*, *Huang* and *Abrams11* share the same local dynamics but have different migration mechanisms. *Mchich* and *ElAbdll.* do not share local dynamics with any other scenario and have to treated separately. In the text and the figures, the labels in the left column (number plus letter, or name) are used to name the scenarios. The letter x, y and z after the number indicates a migration rule where there is no migration loss (x), or where gain and loss are identical, $\nu_x = \rho_x$, which means that all migrating individuals arrive at their destination (y if this applies only to the prey and z if this applies to both species).

Group (1) represents the most general models, for which all exponent parameters have their maximum meaningful range. In group (2), migration is diffusive for both species, but the other local exponent parameters are still the in maximum meaningful range. Models (4) to (7) have a Holling type 2 functional response with logistic growth and no predator interference, and they differ with respect to the migration term. Model (4) *Jans95* shares the local patch dynamics with most of the models in the literature (Rosenzweig-McArthur model(Rosenzweig and MacArthur, 1963)) and has a simple diffusive migration. Model (5) is the same as model (4) but with no prey migration. Model (6R) *Huang* adds that over-abundance of prey facilitates predator migration while model (6) incites predators to stay if there is plenty of food available. Model (7) *Abrams11* lets the prey on the own patch encourage the predator to stay while great numbers of prey on the other patch are an incentive to migrate.

Models (9) and (10) establish a relation between consumption rate and migration: the migration rate of the predator scales in the same way as its feeding rate (i.e., the biomass production), and the migration rate of the prey scales with its own growth rate as well as with the predator feeding rate and with predation on the other patch.

We group all these models into two classes, with class I comprising the models with general intervals for the 5 in-patch scale parameters (models (1), (2), (9)) and class II comprising models (4) to (7) and (10), which are based on the Rosenzweig-MacArthur model.

Models (3) *Mchich* and (8) *ElAbdllaoui* fix more parameters for the in-patch dynamics but have interesting migration rules: *Mchich* lets the prey flee if there are many predators in the own patch. *ElAbdllaoui* additionally makes the predator sedentary if there is plenty of food available.

3. Results

3.1. Proportion of stable systems

We evaluated the proportion of stable states in an ensemble where the scale and exponent parameters were chosen at random from the intervals indicated in Tab. 2. We generated 10^7 random sets of parameters for each model where each parameter was drawn uniformly from the respective intervals. We define the proportion of stable webs (PSW) as the number of parameter sets which produce a stable equilibrium divided by the total number of sets sampled.

At first, we performed this evaluation in the absence of migration (i.e., for single patches), obtaining PSW=0.939 for class I, PSW=0.639 for class II and PSW=0 for *Mchich* and PSW=1 for *ElAbdllaoui*. This establishes the amount of stable webs we can expect purely based on local patch dynamics without interference of migration. We know from Gross et al. (2009) that mortality and feeding terms tend to be positively correlated with stability and growth terms are negatively correlated with stability for local dynamics. This means that high values for γ and $\mu^{x,y}$ and low values for ϕ and ψ should enhance stability. Judging by this knowledge we expect *Mchich* to be less stable than *ElAdbllaoui* and class I to be more stable than class II for purely local dynamics. This is confirmed.

Mchich is special case as the PSW does not necessarily reflect the actual stability. The particular parameter choices of Mchich et al. (2007) create a pair of purely complex conjugate eigenvalues, both for the case with and without migration. This does not allow for a conclusive linear stability analysis and higher order terms are be needed to judge stability of a steady state.

The PSW values are given in Tab. 3, together with the values obtained in the presence of migration. Tab. 3 shows that PSW values are different for different models, ranging from 0.05 for model (10), which has a complex migration rule, to 0.94 for class I with diffusive, conservative migration, i.e., models (2y) and (2z). In class II, the models with diffusive migration are those with the highest stability. In all cases, stability with migration is smaller than or roughly equal to stability without migration.

The conclusions from Tab. 3 are thus that migration is in general destabilizing, with diffusive (i.e. non-adaptive) migration being less destabilizing than other migration rules.

It is interesting to note that the class II systems are less stable than the models with diffusive migration, (2) to (2z), despite the high exponent of closure $\mu_x = 2$. A high exponent of closure is well known to be stabilizing since it implies a strong density limitation of the predator(Plitzko et al., 2012; Gross et al., 2009). In order to investigate the effect of the exponent of closure, we run the class II systems also with $\mu_x = 1$ instead of 2. In this case all systems became unstable. When μ_x was chosen at random from the interval $[1, 2]$, the average stability was lower than for the isolated patches (around 0.50), but with trends similar to those for $\mu_x = 2$.

In order to obtain more detailed information about the effect of migration on stability, we evaluated the correlation of stability with the scale parameters of migration. The result is shown in Fig. 1 .

Scenario	PSW without Migration	PSW with Migration
(1)Stand	0.939	0.227
(1x)Stand	0.939	0.570
(1z)Stand	0.939	0.394
(2)Diff	0.939	0.924
(2x)Diff	0.939	0.876
(2y)Diff	0.939	0.942
(2z)Diff	0.939	0.939
(9)Growth	0.939	0.450
(4)Jans95	0.693	0.693
(4x)Jans95	0.693	0.693
(4z)Jans95	0.693	0.693
(5)Jans01	0.693	0.693
(5z)Jans01	0.693	0.693
(6)Huang	0.693	0.552
(6R)Huang	0.693	0.530
(7)Abrams11	0.693	0.693
(10)Growth2	0.693	0.051
(3)Mchich	0.000	0.00
(3x)Mchich	0.000	0.00
(8)ElAbdllaoui	1.000	0.625

Table 3: The different scenarios and their proportion of stable webs with and without migration. The double horizontal lines separate the classes I, II, and the exceptions *Mchich* and *ElAdbllaoui*.

In most cases, the correlation is zero or negative, and there are only four instances of a significant positive correlation with migration. Positive correlation values mean that higher relative migration rates make the equilibrium more stable, negative correlation values make the equilibrium less stable. It is interesting to note that out of the five instances with positive correlations four are loss terms $\rho_{x,y}$. This fits together with the observation that loss terms are comparable to death terms, which are known to be stabilizing for local dynamics(Gross et al., 2009).

To summarize, the results in Fig. 1 imply that most models become less stable when the contribution of migration to the total gain and loss terms

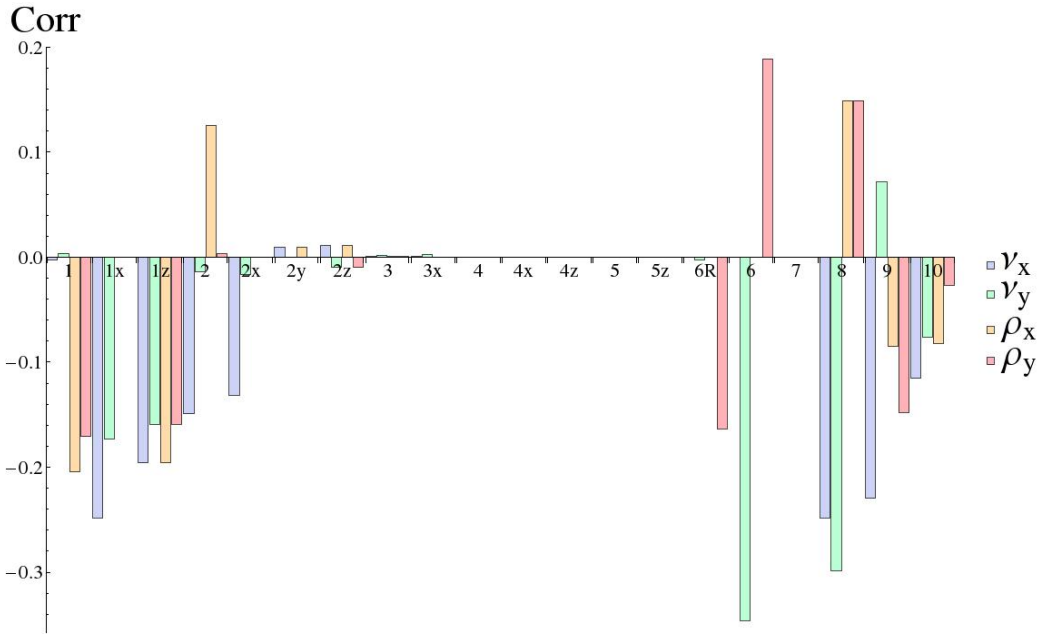

Figure 1: The correlation of the four scale parameters of migration $(\nu_x, \nu_y, \rho_x, \rho_y)$ with stability for 10^7 random parameter samples. The different models are arranged along the x-axis, the correlation value is given along the y axis. The different scale parameters are coded by colour. Most models show a negative correlation of the migration parameters with stability.

increases. However, several models become more stable with increasing migration losses, *ElAbdllaoui*, *Huang* and *Diff*, and only *Growth* becomes more stable with increasing migration gains. The models *ElAbdllaoui*,*Huang* and *Growth* all show types of adaptive migration. The model *Diff* has simple diffusion as a dispersal mechanism though both *Diff* and *Growth* have wide parameter interval ranges for local parameters.

In addition to evaluating the correlation of the scale parameters with stability, we also evaluated how average stability changes as a scale parameter is varied. Example curves that represent the qualitatively different types of behaviour found are shown in Fig. 2.

The top left graph shows a monotonous decrease, which is most often obtained and applies to most scenarios that have a negative correlation of the scale parameter with stability. The bottom right graph shows a monotonous increase, which is seen in the cases of positive correlation of the scale parameters with stability. The bottom left graph shows an instance of a

non-monotonous curve, found for the scenarios *Stand*, *Growth* and *Growth2*, which have complex migration rules, where more than two of the eight migration exponent parameters (ω , κ) are different from zero. This shows that cross-patch cross-species interactions as seen in these three classes can create positive correlation of migration scale parameters with stability within certain ranges even if the overall correlation remains negative. The top right graph is an instance where migration has no effect on stability.

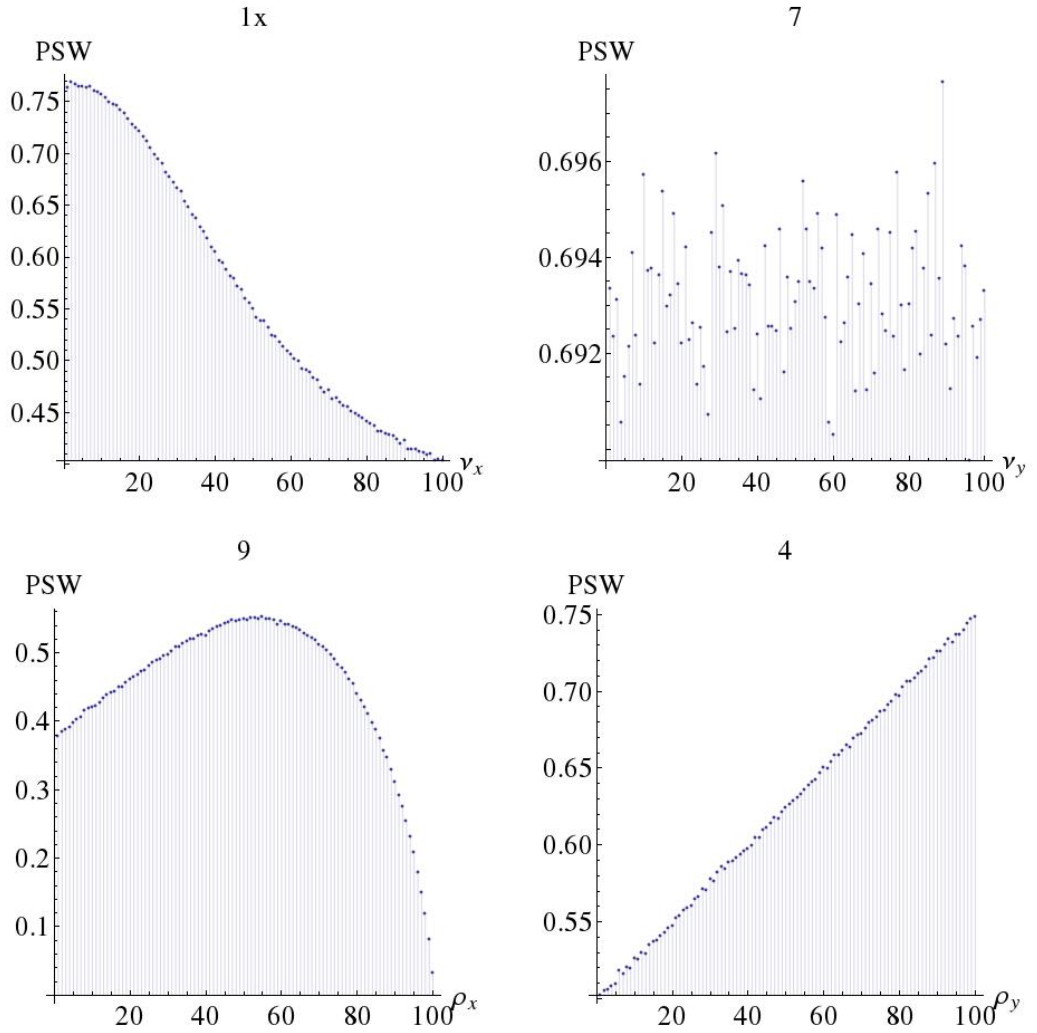

Figure 2: Examples of the different types of functional relation between scale parameters and average stability. The graphs show the proportion of stable systems as function of a migration scale parameter. The numbers above each plot denote the model (see Tab. 2) which is defined by the intervals of the exponent parameters and the relationship between scale parameters used to create the data. Apart from a monotonous decrease or increase, there are also models with a constant proportion of stable systems and those with maxima at intermediate values of the scale parameter.

Inspired by these findings, we investigated additional cases: Instead of linear relationships for the sensitivity of the migration on the respective population ($\omega_{x,y}$=1, as used in class II), we used quadratic relationships ($\omega_{x,y}$=2) for the scenarios of class II. This caused clear trends, with the average stability decreasing with increasing values of the scale parameters $\nu_{x,y}$ and increasing with $\rho_{x,y}$. Even though slope and absolute values vary, this effect dominates over every other influence on stability and shapes the curves almost solely. This is understood by realizing that $\omega_{x,y} = 2$ implies large loss terms at high values of ρ. The dependence on ν is more complicated as ν affects only the non-diagonal elements of the Jacobian matrix. High ν creates larger diagonal elements for the migration sub-matrix. This increases the trace $T(J_+)$ and thus decreases the likelihood of a stable equilibrium even though $T(J_-)$ becomes more stable as the total stability is limited by the stability of each sub-matrix.

3.2. Example of analytical computation

In most cases, the stability curves are not easily understood. The stability condition comprises four inequalities, two for each matrix $L \pm M$ (see paragraph after eq. (18)). Each of these inequalities contains several parameters, and checking whether they are satisfied requires the consideration of a multitude of cases. In the following we demonstrate for the model with the smallest number of free parameters, which is the model *ElAbdllaoui*, how the shape of the stability curve results from the inequalities. As an example we use the average stability versus the scale parameter ν_y, as it has a distinct shape of two linear sections with different slopes.

The traces and determinants for this model are

$$\begin{aligned}
T(J_+) &= 1 - 2(1-\delta)(1-\rho_x) - \delta(1-\rho_x) - \rho_x \,, \\
T(J_-) &= 1 - 2(1-\delta)(1-\rho_x) - \delta(1-\rho_x) - \rho_x - 2\nu_x - 2\alpha_y\nu_y \,, \\
\Delta(J_+) &= -(\delta(-1+\rho_x) - \rho_x + \nu_x)(\alpha_y(1+\rho_y-\nu_y) - \alpha_y\nu_y) \,, \\
\Delta(J_-) &= -2\alpha_y(1 - 2(1-\delta)(1-\rho_x) - \delta(1-\rho_x) - \rho_x - 2\nu_x)\nu_y \,, \\
&\quad -(\delta(-1+\rho_x) - \rho_x - \nu_x)(\alpha_y(1+\rho_y-\nu_y) + \alpha\nu_y) \,.
\end{aligned}$$

The equilibrium is stable if both traces are negative and both determinants are positive. The values of δ, $\rho_{x,y}$ and $\nu_{x,y}$ are in the interval $[0, 1]$. This means that $T(J_{+,-}) < 0$ and $\Delta(J_-) > 0$. The stability is thus solely dependent on

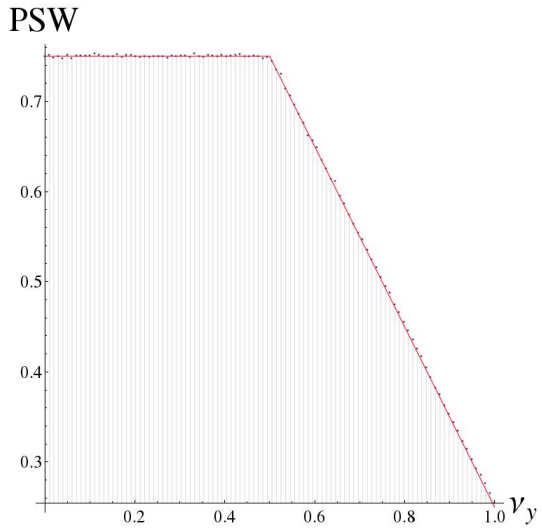

Figure 3: The average stability as a function of ν_y for the scenario *ElAbdllaoui*. The solid red line show the analytical result.

$\Delta(J_-)$. Rewriting $\Delta(J_+)$ as

$$\Delta(J_+) = -\alpha_y f_1 \cdot f_2$$

with $f_1 = \delta(\rho_x - 1) - \rho_x + \nu_x$ and $f_2 = 1 + \rho_y - 2\nu_y$, the stability condition becomes $f_1 f_2 < 0$, which means that f_1 and f_2 must have opposite signs. The term f_1 is independent of ν_y and thus cannot change sign as ν_y is changed. With all parameters in f_1 being random numbers in $[0, 1]$, $f_1 < 0$ in 75% of the cases, and $f_1 > 0$ in 25% of the cases. f_2 is always larger than zero as long as $\nu_y < 0.5$. This means that the equilibrium is stable in 75% of the cases. As ν_y increases from 0.5 to 1, the probability that $f_2 > 0$ drops linearly from 1 to 0. For $\nu_y = 1$, only 25% percent of the systems are stable because now f_1 must be positive. This explains the linear drop of the stability curve from 0.75 to 0.25.

3.3. Bifurcations

We evaluated how often each of the four different types of bifurcations occurs as a migration scale parameter is increased from 0 to 1, averaging over 10^7 parameter sets and over the four different migration scale parameters. The result is shown in Fig. 4.

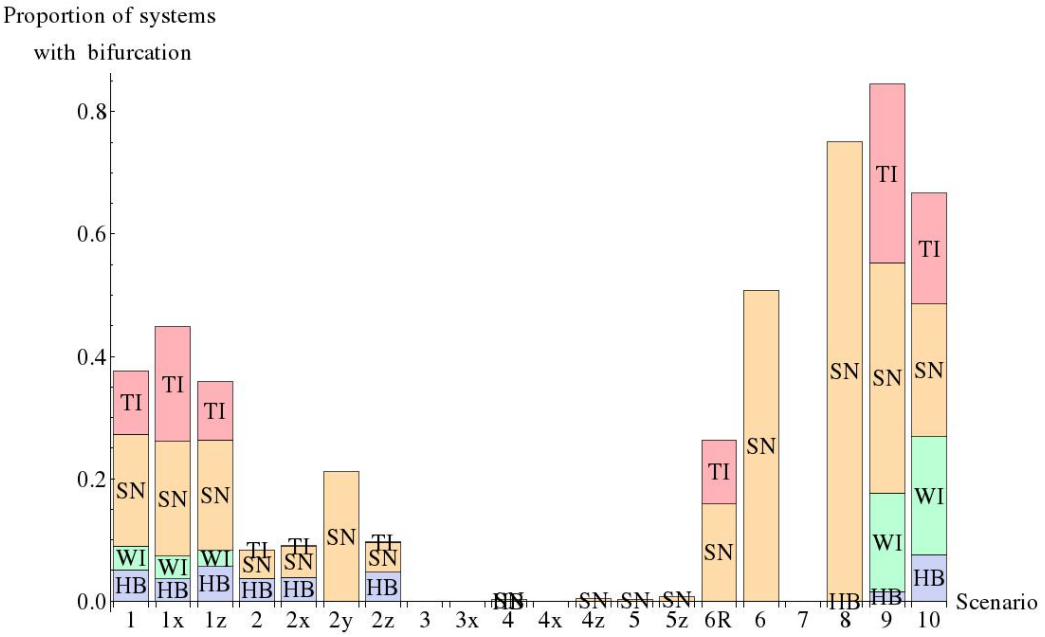

Figure 4: The statistics of the four types of bifurcations for all considered models for 10^5 random parameter sets. The numbers on the x-axis denote the model (see Tab. 2). Since more than one type of bifurcation can occur as a scale parameter is increased from 0 to 1, the maximum total height of each bar is four. The symbols are SN for saddle-node bifurcation, HB for Hopf bifurcation, TI for Turing instability and WI for wave instability.

The dominant bifurcation is always the saddle-node bifurcation. We see all four different types of bifurcations in *Stand* and *Standx* as well as *Growth* and *Growth2*. The models with diffusive migration (*Diff* and *Jans*) do not show wave instabilities. For the scenarios of class II we see barely any bifurcations, with the exception of the models *Huang*,*HuangR* and *Growth2*, though *Huang* only exhibits saddle-node and *HuangR* saddle-node and Turing bifurcations. This is consistent with the earlier analysis of stability. If migration does not cause a change in stability, there can be no bifurcations. Comparing these results with Table 3, we see that there is some correlation between the amount by which migration decreases stability and the number of bifurcations that occur.

By evaluating the bifurcation statistics separately for different intervals of the migration scale parameters, we found that generally Hopf bifurcations and wave instabilities occur more often for intermediate values of the scale parameters, while saddle-node bifurcations and Turing instabilities occur more

often for large and small values. Figs. 5 and 6 show the corresponding histograms for selected models. For these figures, we evaluated additionally the information whether the used parameter set would produce a stable equilibrium without migration, i.e. with all migration scale parameters set to zero. This subset of the total number of bifurcations is marked by the violet colour.

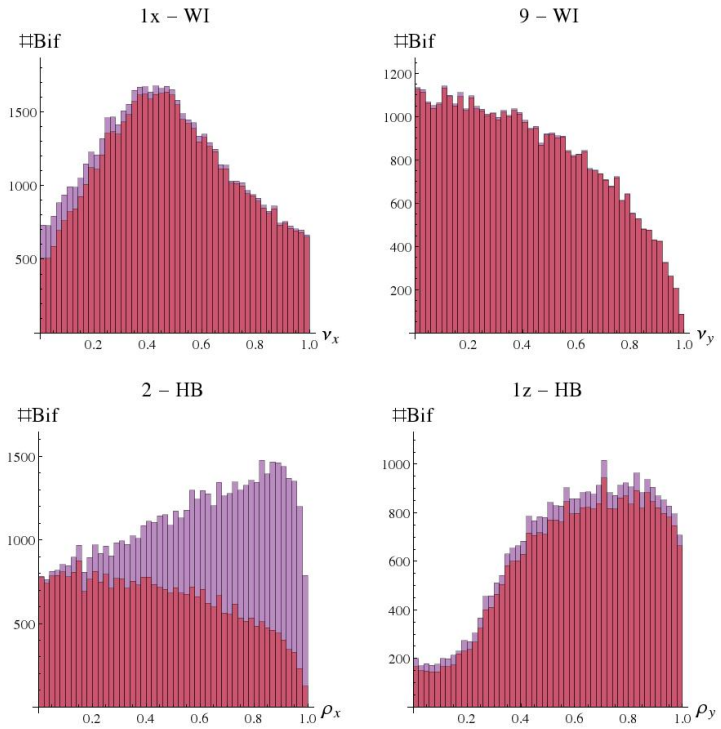

Figure 5: The number of bifurcations into oscillating states in dependence of the migration scale parameters, in a sample of 10^6 random parameter sets. The symbols above each graph denote the model (see Tab. 2) and type of bifurcation("HB" stands for synchronous Hopf bifurcation and "WI" stands for wave instability). The shape in the top left graph with most bifurcations at mid-range values is found for 38 percent of cases. Other forms that are seen less often (predominantly in models with complex migration dynamics) are shown in the other histograms. The darker bars indicate the part of parameter sets with a bifurcation that would have been stable without any migration.

Saddle-node bifurcations are more likely to occur at high migration values, whereas Turing-bifurcations tend to low and mid values. Synchronous Hopf bifurcations are usually found at mid-to-high levels of migration while wave-instabilities prefer mid-to-low migration. If we look specifically at gain and

loss terms we see they do not behave the same for wave instabilities and Turing bifurcations.

It has been noted that prey pursuit or predator evasion can decrease synchrony(Li et al., 2005). The scenarios *ElAbdllaoui*, *Growth* and *Growth2* implement such types of migration. *ElAbdllaoui* shows more synchronous Hopf bifurcations at high values of migration scale parameters. *Growth* and *Growth2* have no clear trend.

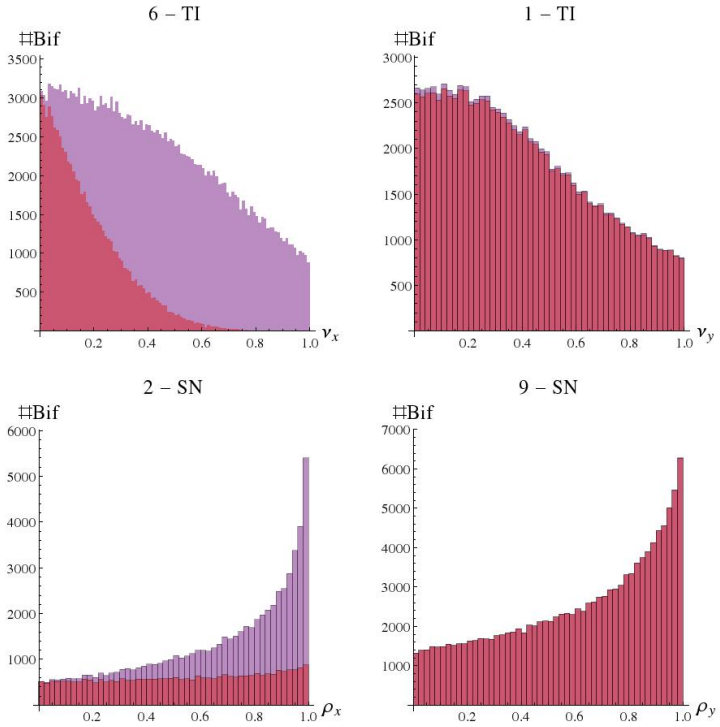

Figure 6: Histograms of the number of saddle-node and Turing bifurcations over migrations scale parameters. The majority of bifurcations occur for scale parameters close to zero or 1. We sampled 10^5 random sets of parameters per model. The number of bifurcations into oscillating states in dependence of the migration scale parameters, in a sample of 10^6 random parameter sets. The symbols above each graph denote the model (see Tab. 2) and type of bifurcation("SN" stands for saddle-node bifurcation and "TI" stands for Turing instability). The majority of bifurcations, 67 percent of total cases, occur for scale parameters close to zero or 1. The darker bars indicate the part of parameter sets with a bifurcation that would have been stable without any migration.

4. Comparison with results from explicit models

Many of the models we studied with generalized modelling listed in Table 2 were investigated earlier using explicit population dynamics models. These are the models by Mchich et al. (2007),Jansen (2001); V.A.A.Jansen (1995), Abdllaoui et al. (2007), Abrams and Ruokolainen (2011) and Huang and Diekmann (2001). In the following, we compare our findings to theirs.

V.A.A.Jansen (1995) sees no dependence of the bifurcation condition on migration for the homogeneous equilibrium with both species present on both patches. In our study, we found (few) bifurcations in this model. We found that this difference is due to the fact that in our study the exponent parameters are chosen independently of the steady state values, while they do depend on them in the model by V.A.A.Jansen (1995). This is true as well for the follow-up paper from 2001(Jansen, 2001). The model of Jansen thus represents a special case of our general formulation. Our results indicate that other models of this class do show bifurcations.

Mchich et al. (2007) find a stabilizing effect of migration. This model uses different time scales for migration and local dynamics and comes to his results by computing dynamics in a "two-step" approach. We find that linear stability analysis produces inconclusive results because it gives a neutrally stable equilibrium. The effects seen by Mchich must thus be due to higher-order terms.

Abdllaoui et al. (2007) use the same two-step approach. They state that migration can create limit cycles. We see a large percentage of stable webs, with Hopf bifurcations occurring only rarely. This suggests that El Abdllaoui et al focussed on the interesting region in parameter space, or that using inhomogeneous systems, as they did, increases the number of Hopf bifurcations.

Abrams and Ruokolainen (2011) state that adaptive migration produces frequent anti-synchronous limit cycles. Scenarios where adaptive migration is a possibility (*Stand*, *Growth*) do produce wave instabilities (and thus anti-synchronous limit cycles). We do not see any bifurcations at all for *Abrams* itself though. This might be a selection issue as *Abrams* only looked at local patch dynamics that produce oscillations which is condition we do not enforce. We also limit our analysis to the homogeneous case and thus exclude any limit cycles that may form out of a heterogeneous equilibrium. While we never see a change of stability with migration, it might very well be that those cases which already are unstable produce populations oscillations that

change between synchronous and anti-synchronous.

Huang and Diekmann (2001) are interested in the effect of handling time on migration with extremes at either no effect and pure diffusion or a strong effect that makes the predator immobile while handling prey and thus migration impossible for sufficient prey concentration. Huang states that there is a stable equilibrium for a wide range of parameters and that there are Hopf bifurcations and wave instabilities, in addition to saddle-node bifurcations. We only find saddle-node bifurcations. This is the case because changing the migration scale parameters alone does not produce Hopf bifurcations. They exist though and can be easily seen by varying one of the local parameters. In fact, changing one parameter in the explicit population dynamical models leads to changes of several of the parameters in the generalized modelling approach, and this then produces Hopf bifurcations also in our approach.

5. Conclusions

We analysed the dynamics of a predator-prey system on two patches that are coupled by migration, using the generalized modelling approach, which is based on linear stability analysis of population dynamics equilibria. We considered 19 different scenarios, each of which is characterized by different ranges of the parameters that characterize the functional dependence of growth and loss terms on the population sizes. Each scenario thus represents a class of models. We computed the average stability, the dependence of stability on migration scale parameters, and the statistics of the four types of bifurcations (saddle-node, Hopf, and the two-patch equivalents of Turing and wave instabilities). Since the stability and the bifurcations follow from analytical expressions, the results can be understood with analytical methods, as we demonstrated for one example.

We found that stability is almost always largest for isolated patches when generalized parameters are averaged over their ranges. Nevertheless, there is a positive correlation of stability with migration scale parameters (i.e. the extent to which population growth and loss terms are dominated by emigration and immigration) within certain ranges in models that use adaptive rules for emigration or immigration rates that depend on the other species and/or the other patch. With random migration, stability is often little or not at all correlated with the migration scale parameters.

We found that all four types of bifurcations can occur in the system as the migration strength is increased. Saddle-node bifurcations are most

frequent. Wave instabilities do not occur with random migration. This was also found by other authors, who used more specific models (Goldwyn and Hastings, 2008; Abrams and Ruokolainen, 2011)). Hopf bifurcations and wave instabilities tend to occur more often for intermediate values of the migration scale parameters.

We were able to confirm and generalize previous results (Gross et al., 2009) about the influence of exponent parameters on the average stability. They found that mortality and feeding terms tend to be positively correlated with stability, and growth terms are negatively correlated with stability. These conclusions, which were obtained for food webs with up to 50 species in the absence of migration, and for parameter intervals that were narrower than ours, agree with our findings. For high (quadratic) sensitivity of migration to the respective population on the respective patch we found that when population gains are dominated by immigration, this has a destabilizing effect, while a domination of losses by emigration has a stabilizing effect. We also found that an exponent of closure close to 2 exerts a stabilizing influence that dominates over the impact of dispersal. This means that migration will rarely destabilize population dynamics models with strong quadratic mortality terms, but it can have a destabilizing effect if predator mortality depends less sensitively on predator density. However, for linear mortality, no stable equilibria are found for any of the scenarios.

Our findings complement those of Tromeur et al. (2013), who studied a metapopulation of one species on many patches using generalized modelling. They found that density-independent dispersal has no effect on stability if the growth term is linear($\phi = 1$), and is destabilizing if growth can saturate ($\phi < 1$). We find that this holds also for the predator-prey system for a Rosenzweig-MacArthur model with density-independent dispersal (e.g. Jansen(Jansen, 2001; V.A.A.Jansen, 1995)) but not for models with other local dynamics (e.g.the model *Diff* defined in this paper), where we see either a weak stabilizing or a destabilizing effect, depending on the relationship between migration gain and loss terms. This means that the addition of a predator can change the effect of dispersal on the stability of a metapopulations.

While the analysis presented in the present paper focusses exclusively on 2-patch systems, we can extrapolate from these results by making use of general insights in the dynamics of networks (Do et al., 2012; MacArthur et al., 2008). Let us first discuss the local instabilities, corresponding to saddle-node and Hopf bifurcations. Since these instabilities emerge from

intra-node dynamics they will be observed almost identically in large complex networks. Nevertheless some caveats apply as in larger networks the high number of dispersal links per node lends more weight to dispersal. Hence it effectively constitutes a rescaling of the local parameters, making the system even more sensitive to the dispersal parameters. Secondly, in networks with a heterogeneous number of dispersal links per node certain dispersal rules will lead to a heterogeneous distribution of the population in even in the steady state. For these types of dispersal already a heterogeneous network of identical nodes will behave as heterogeneous networks. Heterogeneity is likely to lead to systems in which the effect of bifurcations is confined to few habitat patches at a time.

The effect of network structure on pattern-forming instabilities is much more pronounced. Consider for instance that a system-wide anti-phase oscillation is only possible in bipartite networks (networks in which the nodes can be coloured with two colours such that no nodes of the same colour are adjacent). Since large networks are rarely bipartite, this precludes system-wide anti-phase oscillations. However, slightly different Turing and wave instabilities can still occur. In networks of identical or similar patches we can expect that these instabilities originate from symmetrical structures in the network (Do et al., 2012). The respective symmetries are then reflected in the the dynamics. For instance a simple mirror symmetry as in the 2-patch system gives rise to anti-phase oscillations, while a triangle of patches may generate a three-phase oscillation. Hence we expect completely asymmetric networks to be particularly stable.

Acknowledgements

We thank Eric Tromeur for helping with the initial literature search and Andreas Brechtel for useful discussions and cross checking computational data. This work was supported by DFG under contract number Dr300/12-1.

References

Abdllaoui, A. E., Auger, P., Kooi, B. W., de la Parra, R. B., Mchich, R., 2007. Effects of density-dependent migrations on stability of a two-patch predatorprey model. Mathematical Biosciences 210 (1), 335 – 354.
URL http://www.sciencedirect.com/science/article/pii/S0025556407000557

Abrams, P. A., Ruokolainen, L., 2011. How does adaptive consumer movement affect population dynamics in consumerresource metacommunities with homogeneous patches? Journal of Theoretical Biology 277 (1), 99 – 110.
URL http://www.sciencedirect.com/science/article/pii/S0022519311001214

Amarasekare, P., 2008. Spatial dynamics of foodwebs. Annual Review of Ecology, Evolution, and Systematics, 479–500.

Armsworth, P. R., Roughgarden, J. E., 2008. The structure of clines with fitness-dependent dispersal. The American Naturalist 172 (5), 648–657.

Briggs, C. J., Hoopes, M. F., 2004. Stabilizing effects in spatial parasitoid–host and predator–prey models: a review. Theoretical population biology 65 (3), 299–315.

Do, A.-L., Höfener, J., Gross, T., 2012. Engineering mesoscale structures with distinct dynamical implications. New Journal of Physics 14 (11), 115022.

Esa Ranta, V. K., Lundberg, P., 1998. Population variability in space and time: The dynamics of synchronous population fluctuations. Oikos 83, 376–382.

Goldwyn, E. E., Hastings, A., 2008. When can dispersal synchronize populations? Theoretical population biology 73 (3), 395–402.

Gross, T., Feudel, U., Jan 2006. Generalized models as a universal approach to the analysis of nonlinear dynamical systems. Phys. Rev. E 73, 016205.
URL http://link.aps.org/doi/10.1103/PhysRevE.73.016205

Gross, T., Rudolf, L., Levin, S. A., Dieckmann, U., 2009. Generalized models reveal stabilizing factors in food webs. Science 325 (5941), 747–750.

Hanski, I. A., Gaggiotti, O. E., 2004. Ecology, genetics and evolution of metapopulations. Academic Press.

Holland, M. D., Hastings, A., 2008. Strong effect of dispersal network structure on ecological dynamics. Nature 456 (7223), 792–794.

Huang, Y., Diekmann, O., 2001. Predator migration in response to prey density: what are the consequences? Journal of mathematical biology 43 (6), 561–581.

Jansen, V. A., 2001. The dynamics of two diffusively coupled predatorprey populations. Theoretical Population Biology 59 (2), 119 – 131.
URL http://www.sciencedirect.com/science/article/pii/S0040580900915065

Jansen, V. A., de Roos, A. M., 2000. The role of space in reducing predator-prey cycles. The geometry of ecological interactions: simplifying spatial complexity, 183–201.

Koelle, K., Vandermeer, J., 2005. Dispersal-induced desynchronization: from metapopulations to metacommunities. Ecology Letters 8 (2), 167–175.

Leibold, M. A., Holyoak, M., Mouquet, N., Amarasekare, P., Chase, J., Hoopes, M., Holt, R., Shurin, J., Law, R., Tilman, D., et al., 2004. The metacommunity concept: a framework for multi-scale community ecology. Ecology letters 7 (7), 601–613.

Li, Z.-z., Gao, M., Hui, C., Han, X.-z., Shi, H., 2005. Impact of predator pursuit and prey evasion on synchrony and spatial patterns in metapopulation. Ecological Modelling 185 (2), 245–254.

Liebhold, A., Koenig, W. D., Bjrnstad, O. N., 2004. Spatial synchrony in population dynamics*. Annual Review of Ecology, Evolution, and Systematics 35 (1), 467–490.
URL http://dx.doi.org/10.1146/annurev.ecolsys.34.011802.132516

MacArthur, B. D., Sánchez-García, R. J., Anderson, J. W., 2008. Symmetry in complex networks. Discrete Applied Mathematics 156 (18), 3525–3531.

Mchich, R., Auger, P., Poggiale, J.-C., 2007. Effect of predator density dependent dispersal of prey on stability of a predatorprey system. Mathematical Biosciences 206 (2), 343 – 356, arino Special Issue.
URL http://www.sciencedirect.com/science/article/pii/S0025556405002087

Pascual, M., Dunne, J. A., 2005. Ecological networks: linking structure to dynamics in food webs. Oxford University Press.

Pillai, P., Gonzalez, A., Loreau, M., 2011. Metacommunity theory explains the emergence of food web complexity. Proceedings of the National Academy of Sciences 108 (48), 19293–19298.

Plitzko, S. J., Drossel, B., Guill, C., 2012. Complexity–stability relations in generalized food-web models with realistic parameters. Journal of theoretical biology 306, 7–14.

Ristl, K., Plitzko, S. J., Drossel, B., 2014. Complex response of a food-web module to symmetric and asymmetric migration between several patches. Journal of theoretical biology 354, 54–59.

Rooney, N., McCann, K. S., 2012. Integrating food web diversity, structure and stability. Trends in ecology & evolution 27 (1), 40–46.

Rosenzweig, M. L., MacArthur, R. H., 1963. Graphical representation and stability conditions of predator-prey interactions. American Naturalist, 209–223.

Rowell, J. T., 2010. Tactical population movements and distributions for ideally motivated competitors. The American Naturalist 176 (5), 638–650.

Thompson, R. M., Brose, U., Dunne, J. A., Hall, R. O., Hladyz, S., Kitching, R. L., Martinez, N. D., Rantala, H., Romanuk, T. N., Stouffer, D. B., et al., 2012. Food webs: reconciling the structure and function of biodiversity. Trends in ecology & evolution 27 (12), 689–697.

Tromeur, E., Rudolf, L., Gross, T., 2013. Impact of dispersal on the stability of metapopulations. arXiv preprint arXiv:1305.2769.

V.A.A.Jansen, 1995. Regulation of predator-prey systems through spatial interactions a possible solution to the paradox of enrichment. Oikos 74, 384–390.

Yeakel, J., Stiefs, D., Novak, M., Gross, T., 2011. Generalized modeling of ecological population dynamics. Theoretical Ecology 4 (2), 179–194.
URL `http://dx.doi.org/10.1007/s12080-011-0112-6`

va Kisdi, 2010. Costly dispersal can destabilize the homogeneous equilibrium of a metapopulation. Journal of Theoretical Biology 262 (2), 279 – 283. URL http://www.sciencedirect.com/science/article/pii/S0022519309004706